



Equilibrium, Kinetics and Optimization Studies on the Bleaching of Palm Oil Using Activated Karaworo Kaolinite

Ikechukwu A. Nnanwube^{1*}, Okechukwu D. Onukwuli², Vincent N. Okafor², John I. Obibuenyi¹, Regina O. Ajemba², Chinemelum C. Chukwuka³

¹Department of Chemical Engineering, Madonna University, Akpugo, Nigeria.

²Department of Chemical Engineering, Nnamdi Azikiwe University, Awka, Nigeria.

³Department of Chemical Engineering, Chukwuemeka Odimegwu Ojukwu University, Uli, Nigeria

Received 18 March 2020,
Revised 13 Sept 2020,
Accepted 14 Sept 2020

Keywords

- ✓ Bleaching,
- ✓ Clay,
- ✓ Isotherm,
- ✓ Kinetics,
- ✓ Optimization.

ik.nnanwube@gmail.com ;
Phone: +2348136140312;

Abstract

The bleaching efficiency of Karaworo kaolinite activated with hydrochloric acid has been investigated. The clay was characterized by X-ray fluorescence and Fourier transform infrared spectroscopy. The bleaching properties of the clay were investigated by varying the clay dosage, acid concentration and bleaching temperature. A maximum bleaching efficiency of 78.2 % was achieved at the optimum conditions. Equilibrium studies revealed that the Freundlich isotherm model gave better fitting than other models. Kinetic studies revealed that the pseudo-second order kinetic model fitted the adsorption data. Diffusion studies revealed that the intra-particle diffusion is not the sole determinant of the bleaching mechanism. Optimization studies revealed that about 88.26% pigments removal was predicted using response surface methodology, while 82.59% removal was predicted with genetic algorithm.

1. Introduction

Bleaching is an important step in the refining of fats and vegetable-animal oils for industrial applications. In edible oil processing bleaching is responsible for clarified oil that is more stable and also more attractive to the consumer. Clarification is usually carried out in an adsorption process which preferentially uses acid-activated clays to remove undesirable oil components. Bleaching primarily removes coloring pigments such as chlorophylls and carotenes but peroxides and other impurities such as soap, trace pro-oxidant metals and phosphatides are also important targets of the bleaching process. Such light-colored oil influences consumers' preferences but are also beneficial for quality and stability [1].

Studies on the bleaching of palm oil using activated clays have been carried out by a number of authors. Lacin et al. [2] produced activated clay using bentonites collected from Arguvan and Kursunlu, Turkey. Activation was carried out with HCl concentrations varying from 1 to 5 N at the temperature of 95 °C ±1 °C with solid to liquid ratio of 0.1 - 0.5 g.mL⁻¹ and contact time of 2-6 h. The specific surface areas of both Arguvan and Kursunlu bentonites increased after activation. Optimum conditions on the

bleaching capacities of Arguvan and Kursunlu bentonites on cotton oil were determined as 99.99 % and 48.5 %, respectively. Nwabanne [3] studied the mechanism of decolourization of crude palm oil using local clay obtained from Nteje town in Anambra State, Nigeria. Chemical activation of the clay was done using sulphuric acid of 1M concentration. The effect of parameters such as time, temperature, particle size and dosage on the bleaching of palm oil was investigated. It was found that bleaching efficiency increased with increase in time, temperature and dosage, and decreased with increase in particle size.

Response surface methodology (RSM) is a statistical method that uses quantitative data from appropriate experiments to determine regression model equations and operating conditions [4]. It defines the effect of the independent variables, alone or in combination, in the processes [5]. In addition, the methodology also generates a mathematical model [6]. Genetic algorithms are a type of optimization algorithm, used to find the optimal solution(s) to a given computational problem that maximizes or minimizes a particular function. On the other hand, genetic algorithms represent one branch of the field of study called evolutionary computation, in that they imitate the biological processes of reproduction and natural selection to solve for the fittest solutions [7]. Like in evolution, many of a genetic algorithm's processes are random; however, this optimization technique allows one to set the level of randomization and the level of control [7]. Genetic algorithm has been found to be an efficient optimization tool. It has been applied in the optimization of biodiesel production [5, 8], software testing [9], and credit risk assessment [10].

The kinetics of pigments removal from palm oil using clay minerals had been reported [11, 12]. However, there is no reported work known to the authors on the application of genetic algorithm in modeling palm oil bleaching using Karaworo kaolinite. In the present study, the potential of clay obtained from Karaworo in Kogi state of Nigeria as an adsorbent for the removal of pigments from palm oil was studied. The influence of clay dosage, acid concentration, and temperature on pigment removal was studied. The process parameters were optimized using response surface methodology and genetic algorithm. Isotherm studies were carried out using the Langmuir, Freundlich, Temkin and Dubinin-Radushkevich isotherm models. The error analysis of the isotherm models was performed using statistical parameters such as average relative error (ARE), root mean square error (RMSE), Marquardt's percent standard deviation (MPSD) and standard deviation of relative error (S_{RE}). The pseudo-first order, pseudo-second order, Elovich, and Avrami models were deployed to study the sorption kinetics. Diffusion test was performed using the intra-particle diffusion model.

2. Material and Methods

2.1 Materials

The clay sample used in this research was sourced from Karaworo town (Lat:7°15'N; Long 6°50' E) in Kogi State of Nigeria. The crude palm oil was bought from local oil mill at Ezema village, Ojoto in Idemili South local government area, Anambra State, Nigeria.

2.2 Methods

2.2.1 Clay preparation and activation

The clay was dried under the sun at an ambient temperature of 35 °C to make them suitable for grinding. The clay sample was then pulverized and sieved to a particle of 300 µm. 50 g of the clay sample was mixed with 250 mL of the prepared HCl solution. The resulting suspension was heated on a magnetically stirred hot plate at a temperature of 98 °C for 2.0 hours. The acid/clay solution was allowed to cool and then filtered with a filter paper placed on a funnel to recover the clay. The recovered clay was washed

several times with distilled water until a neutral point was obtained after testing the filtrate with pH meter. The clay was then dried at a temperature of 110 °C for 3 hours, ground and sieved with 75µm sieve and stored in desiccators for further use [11, 12].

2.2.2 Characterization

The Kaolinite sample was characterized using the X-ray fluorescence (XRF), Fourier Transform Infrared (FTIR) spectrophotometer, bulk density, surface area, acidity, pH, cation exchange capacity, and oil retention. An ARL 9400XP+ Wavelength-dispersive XRF Spectrometer with a Rh source was used for the XRF analysis of the clay sample. The NBSGSC fundamental parameter program was used for matrix correction of major elements, as well as Cl, Co, Cr, V, Sc, and S. The Rh Compton peak ratio method was used for the other trace elements. Samples were dried and fired at 1000 °C to determine the percentage loss on ignition; for the samples this was less than 2 %. Major element analyses were carried out on fused beads. A pre-fired sample of 1 g and 6 g of lithium tetra-borate flux was mixed in a 5 % Au/Pt crucible and fused at 1000 °C in a muffle furnace, with occasional swirling. The glass disk was transferred into preheated Pt/Au mould and the bottom surface was analyzed.

The infrared spectra were recorded in the mid-infrared region (400-4500 cm⁻¹) in an evacuated chamber of Shimadzu FTIR-8400S spectrophotometer using potassium bromide (KBr) discs as matrices. A spectral resolution of 2 cm⁻¹ was used and spectra were accumulated over 32 scans. The FTIR spectroscopy was applied to all samples. Only 2 mg of each sample was mixed with 100 mg of KBr and pressed under 6 tonnes for 2 minutes in making disk. At first the samples were crushed and ground before making the KBr pellets. The fitting of peaks and smoothing were done with OPUS 2000 software on the Shimadzu 8400S over the working window, 400-4500 cm⁻¹.

2.2.3 Bleaching Experiment

The bleaching experiments were carried out in a batch process. 100 g of the raw (unbleached) palm oil was measured out with a beaker and then poured into a 250 mL flat-bottomed flask. 2 g of the activated clay sample was then added to the flask. The flask was fitted with a condenser to avoid losses through evaporation. The mixture was heated to a temperature of 80 °C for 30 minutes and allowed to cool. The oil and clay mixture was then filtered under gravity using Whatman filter paper and the absorbance was measured. The bleaching efficiency of the activated clay samples was then determined by measuring the colour of the bleached oil using UV-VIS Spectrophotometer (Model WFJ 525) at 450 nm. The above experimental procedure was repeated at different values of the process parameters, such as 1 g, 2 g, 3 g, 4 g, and 5 g clay dosage, time of 5 - 80 minutes at 5 minutes interval, temperature of 70, 80, 90, and 100 °C; and acid concentration of 1, 3, 5, 7, 8, and 9 M to determine their influence on the bleaching efficiency [11, 12]. The bleaching efficiency is defined by the following expression in Equation (1).

$$\text{Bleaching efficiency (\%)} = \frac{A_u - A_b}{A_u} \times 100 \quad (1)$$

The relative amount of pigment adsorbed (X) is obtained from Equation (2):

$$X = \frac{A_u - A_t}{A_u} = 1 - \frac{A_t}{A_u} = 1 - X_e \quad (2)$$

The amount of pigment adsorbed at time t per unit mass of clay, q_t (mg/g), is given by Equation (3):

$$q_t = \frac{X}{m} \quad (3)$$

where A_u and A_b are absorbencies of unbleached and bleached palm oil respectively, at 450 nm. A_t is the absorbance of bleached oil at time t. X_e is the residual relative amount at equilibrium, while m is the mass of the clay. For equilibrium studies, X_e is taken to be equal to C_e .

2.2.4 Estimation of isotherm parameters by non-linear regression

Due to the bias arising from linearization, non-linear regression was deployed to determine alternative isotherm parameter sets. This helps to avoid error in choosing isotherm model that fits the experimental data [13]. In doing this, four equations were used to perform the error analysis. The error functions employed are shown in Equations (4-7):

(i) The average relative error (ARE):

$$ARE = \frac{100}{n} \sum_{i=1}^n \left| \frac{q_{e,exp} - q_{e,cal}}{q_{e,exp}} \right| \quad (4)$$

(ii) The residual root mean square error (RMSE):

$$RMSE = \sqrt{\frac{1}{n-2} \sum_{i=1}^n (q_{e,exp} - q_{e,cal})^2} \quad (5)$$

(iii) Marquardt's percent standard deviation (MPSD):

$$MPSD = 100 \sqrt{\frac{1}{n-p} \sum_{i=1}^n \left(\frac{q_{e,exp} - q_{e,cal}}{q_{e,exp}} \right)^2} \quad (6)$$

(iv) Standard deviation of relative error (S_{RE}):

$$S_{RE} = \sqrt{\frac{\sum_{i=1}^n [(q_{e,exp} - q_{e,cal}) - ARE]^2}{n-1}} \quad (7)$$

where n is the number of data points, p is the number of parameters in each isotherm model, $q_{e,exp}$ and $q_{e,cal}$ (mg g^{-1}) are the respective experimental and calculated equilibrium adsorption capacity values.

2.2.5 Design of Experiment

The process variables that influence the removal of pigments from palm oil were investigated using RSM combined with five-level, three-factor factorial design as established by Design Expert software 10.0 trial version (Stat-Ease Inc., Minneapolis, USA). The process variables were bleaching temperature, bleaching time, and clay dosage. The response variable was chosen as bleaching efficiency. The factor levels were coded as $-\alpha$, -1 , 0 , $+1$ and $+\alpha$. The range and levels are shown in Table 1. The experiments were performed randomly to avoid systemic error. The results were analyzed using the analysis of variance (ANOVA), model summary statistics and response surface plots. In RSM, the most widely used second-order polynomial equation developed to fit the experimental data and identify the relevant model terms is shown in Equation 8.

$$Y = \beta_0 + \sum_{i=1}^n \beta_i x_i + \sum_{i=1}^{n-1} \sum_{j=2}^n \beta_{ij} x_i x_j + \sum_{i=1}^n \beta_{ii} x_i^2 + \varepsilon \quad (8)$$

where Y is the predicted response variable which is the bleaching efficiency in this study, β_0 is the constant coefficient, β_i is the i th linear coefficient of the input variable x_i , β_{ii} is the i th quadratic coefficient of the input variable x_i , β_{ij} is the different interaction coefficients between the input variables x_i and x_j and ε is the error of the model.

Table 1: Levels of independent variables for CCD experimental design.

Independent variable	Unit	Symbol	Coded variable levels				
			$-\alpha$	-1	0	+1	$+\alpha$
Temperature	°C	A	19.7731	30	45	60	70.2269
Time	min	B	3.1821	10	20	30	36.8179
Dosage	g	C	0.8182	1.5	2.4	3.5	4.1818

3. Results and Discussion

3.1 XRF analysis

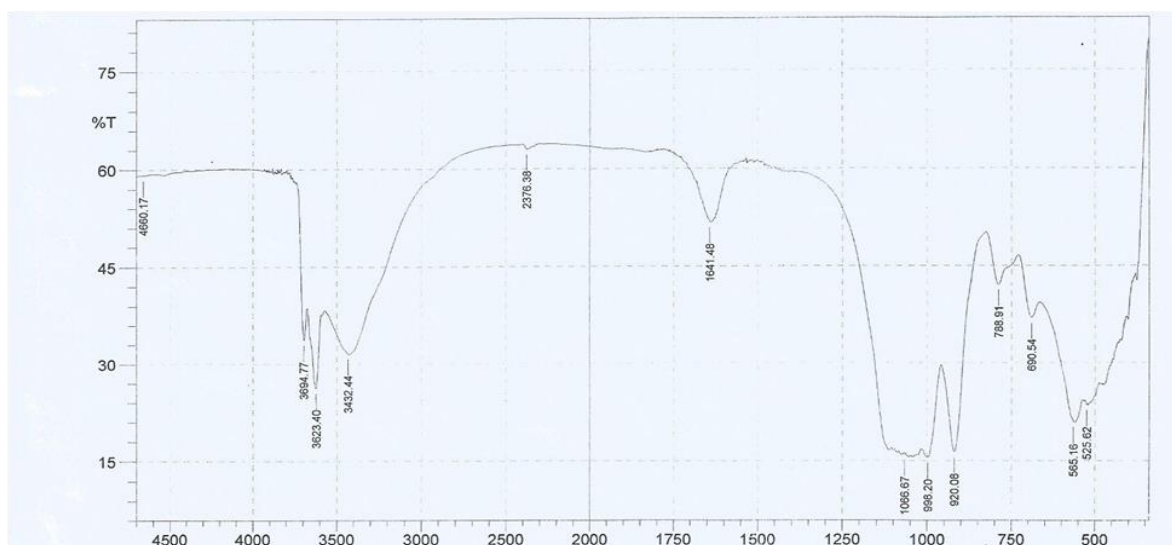
The result of XRF analysis of Karaworo clay shown in Table 2 reveals that alumina (Al_2O_3), hematite (Fe_2O_3), and Quartz (SiO_2) are present in major quantities. TiO_2 and Rh_2O_3 are present in minor quantities while other components are present in traces. About 14.61% loss on ignition was recorded. The result shows that the clay exists mainly as aluminosilicate.

Table 2: XRF result of Karaworo kaolinite.

Oxides	Percentage (%)	Oxides	Percentage (%)	Oxides	Percentage (%)
Al_2O_3	14.1	V_2O_5	0.29	ZnO	0.03
SiO_2	57.00	Cr_2O_3	0.10	MoO_3	0.20
Fe_2O_3	8.643	Mn_2O_3	0.01	Rh_2O_3	1.11
SO_3	0.05	P_2O_5	0.30	Re_2O_7	0.20
CaO	0.20	NiO	0.19	IrO_2	0.22
TiO_2	2.70	CuO	0.045		

3.2 FTIR analysis

The FTIR spectra of Karaworo kaolinite is presented in Figure 1. The result showed the functional groups present in the clay. The band at 525 cm^{-1} is attributed to C-C=O bend and C-I stretch while the band at 565 cm^{-1} is attributed to Si-O-Al stretch.

**Figure 1:** FTIR spectra of Karaworo kaolinite.

The band at 690 cm^{-1} is attributed to C-S stretch and CH out-of-plane deformation while the band at 788 is attributed to Si-C stretch and Si-O bend. The band at 920 cm^{-1} is attributed to Al-O-Si stretch while the band at 998 cm^{-1} is attributed to Si-O-Si stretch. The band at 1066 cm^{-1} is attributed to Si-O-Si anti-symmetrical stretch while the band at 1641 cm^{-1} is attributed to C=N, C=O, and Al-O-H stretches while the band at 2376 cm^{-1} is also attributed to Al-O-Si stretch. The bands at 3623 cm^{-1} and 3694.77 cm^{-1} are attributed to OH stretch for dilute solution.

3.3 Physical characterization

The physical properties of the raw and activated kaolinite sample used as adsorbent are given in [Table 3](#). The result shows that the bulk density, pH, and cation exchange capacity of the clay decreased upon activation, while the oil retention, surface area and acidity increased after activation.

Table 3: Physical properties of the raw and activated Karaworo kaolinite.

Property	Karaworo kaolinite	
	Raw	Activated
Bulk density (g/cm^3)	988.4	764.3
Oil retention (%)	24	56
Surface area (m^2/g)	79.4	279.3
Acidity	0.011	0.02
pH	5.4	3.01
CEC (meg/100g)	91	54

3.4 Effect of process variables on bleaching efficiency

The effect of process variables such as the acid concentration during clay activation, clay dosage, and temperature were examined as these properties determine the extent of pigments removal from palm oil.

3.4.1 Effect of acid concentration on the bleaching efficiency

The effect of acid concentration on the bleaching efficiency of Karaworo clay is shown in [Figure 2](#). Clay dosage was kept constant at 3 g. The result shows that the bleaching efficiency of the clay sample measured by the percentage colour reduction increased with increase in acid concentration.

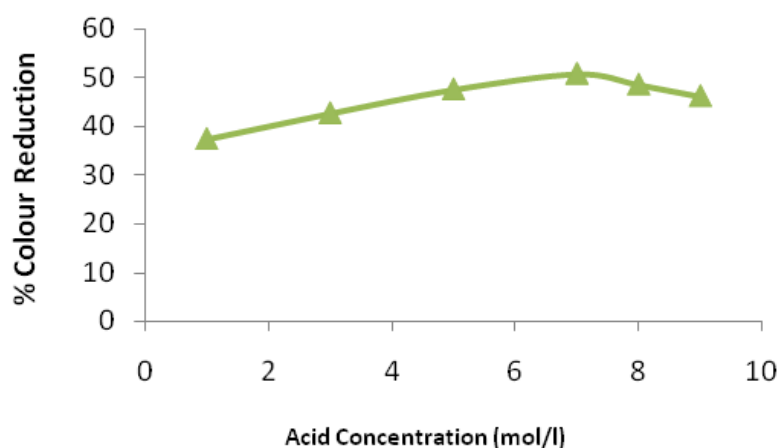


Figure 2: Effect of the concentration of HCl on bleaching efficiency of Karaworo kaolinite.

The increase in the colour reduction advanced towards a maximum, above which the bleaching efficiency decreased. This could be credited to the total destruction of the clay structure at higher acid concentration [11]. A maximum concentration of 7.0 mol/L was recorded for Karaworo clay activation

with percentage colour reduction of 50.8%. Beyond this, further increase in concentration reduced the colour reduction capacity of the clay.

3.4.2 Effect of clay dosage on the percentage colour reduction

The result on the effect of clay dosage on the percentage colour reduction is shown in Figure 3. Acid concentration was kept constant at 7 M. The result showed that as the clay dosage increased, the colour reduction efficiency increased; though the colour reduction efficiency decreased as the clay dosage was increased beyond 4 g. This could be linked to the fact that as adsorption progresses, the active sites available in the clay particles are being occupied by adsorbed particles which block further adsorption, thereby reducing the extent at which colour pigments are removed from the oil. This observation was also supported by Bakhtyar et al. [14].

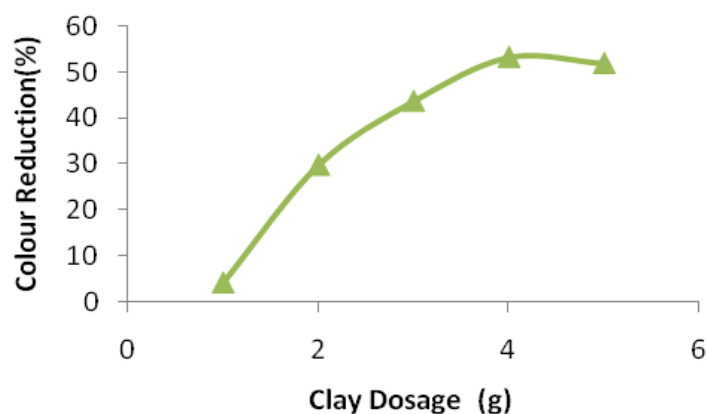


Figure 3: Plot of percentage colour reduction versus clay dosage for Karaworo kaolinite using 7M HCl.

3.4.3 Effect of temperature on the bleaching efficiency

The effect of temperature on the bleaching efficiency of Karaworo kaolinite activated with hydrochloric acid is shown in Figure 4. The results indicate that the percentage of colour pigments adsorbed by the activated clay sample increased as the temperature increased from 70 °C to 100 °C, indicating an endothermic adsorption process. This trend might be attributed to the increase in the rate of diffusion of the adsorbate molecules across the external boundary layer and in the internal pores of the adsorbent particle, due to the decrease in the viscosity of the solution [15].

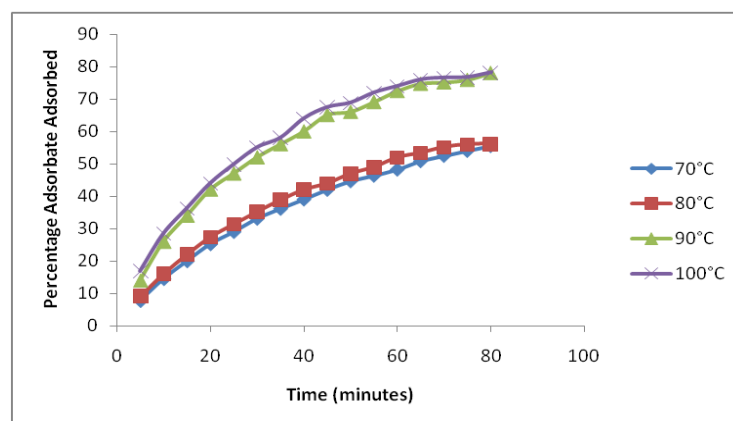


Figure 4: Effect of temperature on the percentage pigments removed using Karaworo kaolinite activated with HCl.

3.5 Bleaching kinetics

The kinetics of pigments removal from palm oil using activated Karaworo clay was investigated with the aid of kinetic models such as pseudo-first order [15], pseudo-second order [15], Elovich [15] and

Avrami [16] models. The linear and non-linear forms of the models are as shown in Table 4. The mechanism of the bleaching process was studied using the intra-particle diffusion model [17]

Table 4: Kinetic models fitted to pigments adsorption.

Model	Non-linear form	Linear form
Pseudo first order	$q_t = q_e(1 - \exp(-k_1t))$	$\log(q_e - q_t) = \log q_e - \frac{k_1}{2.303} t$
Pseudo second order	$q_t = \frac{K_2 q_e^2 t}{1 + k_2 q_e t}$	$\frac{t}{q_t} = \frac{1}{k_2 q_e^2} + \frac{t}{q_e}$
Elovich	$q_t = \frac{1}{\beta} \ln(1 + \alpha\beta t)$	$q_t = \frac{1}{\beta} \ln(\alpha\beta) + \frac{1}{\beta} \ln t$
Avrami	$q_t = q_e \{1 - \exp[-(K_{AV}t)]^{n_{AV}}\}$	$\ln \ln\left(\frac{q_e}{q_e - q_t}\right) = n_{AV} \ln K_{AV} + n_{AV} \ln t$
Intra-particle diffusion	-	$q_t = K_{id} t^{\frac{1}{2}} + c$

The corresponding kinetic parameters have been estimated from the slopes and intercepts of the respective linear plots of the kinetic equations, and the values are shown in the Table 5.

Table 5: Kinetic parameters of different kinetic models at different temperatures for pigment adsorption unto activated Karaworo kaolinite

Kinetic models	Parameters	Temperature (°C)			
		70	80	90	100
Pseudo-first-order	$k_1(\text{min}^{-1})$	0.041	0.058	0.046	0.053
	q_e (mg/g)	0.708	0.953	0.938	0.991
	R^2	0.937	0.840	0.973	0.970
Pseudo-second-order	$k_2(\text{g/mg.min})$	1.96×10^{-2}	2.37×10^{-2}	2.64×10^{-2}	3.34×10^{-2}
	q_e (mg/g)	0.931	0.907	1.117	1.071
	R^2	0.999	0.997	0.998	0.997
Elovich	α (mg/g.min)	0.041	0.046	0.072	0.082
	β (g/mg)	5.464	5.348	4.098	4.167
	R^2	0.976	0.980	0.991	0.990
Avrami	k_{AV}	3.28×10^{-2}	3.95×10^{-2}	3.97×10^{-2}	4.45×10^{-2}
	n_{AV}	1.114	1.178	1.056	1.053
	R^2	0.983	0.955	0.988	0.982

From Table 5, the average calculated coefficient of determination (R^2) for the pseudo-second order model is higher (0.998) compared to those of pseudo-first order (0.930), Avrami model (0.977) and Elovich model (0.984). This suggests that the pseudo-second order model describes the adsorption kinetics of the present system better than other models. The non-linear plots of the kinetic models with the experimental values at various temperatures are shown in Figure 5.

3.6 Mechanism of bleaching

The intra-particle diffusion plays an important role in understanding the mechanisms and rate controlling steps affecting the kinetics of adsorption/bleaching. From intra-particle diffusion model shown in Table 4, the plot of q_t against $t^{0.5}$ should be linear if intra-particle diffusion is involved in the adsorption process and if these lines pass through the origin, then intra-particle diffusion is the rate controlling step. When the plots do not pass through the origin, it indicates that the boundary layer has some degree of control and further shows that the intra-particle diffusion is not the only rate limiting step, but other kinetic models may also control the rate of adsorption, all of which may be operating simultaneously [16]. In the present study, the plots of q_t against $t^{0.5}$ (figure not shown) do not pass through the origin, showing that intra-particle diffusion is not the only rate controlling step. The intra-particle diffusion parameters are shown in Table 6.

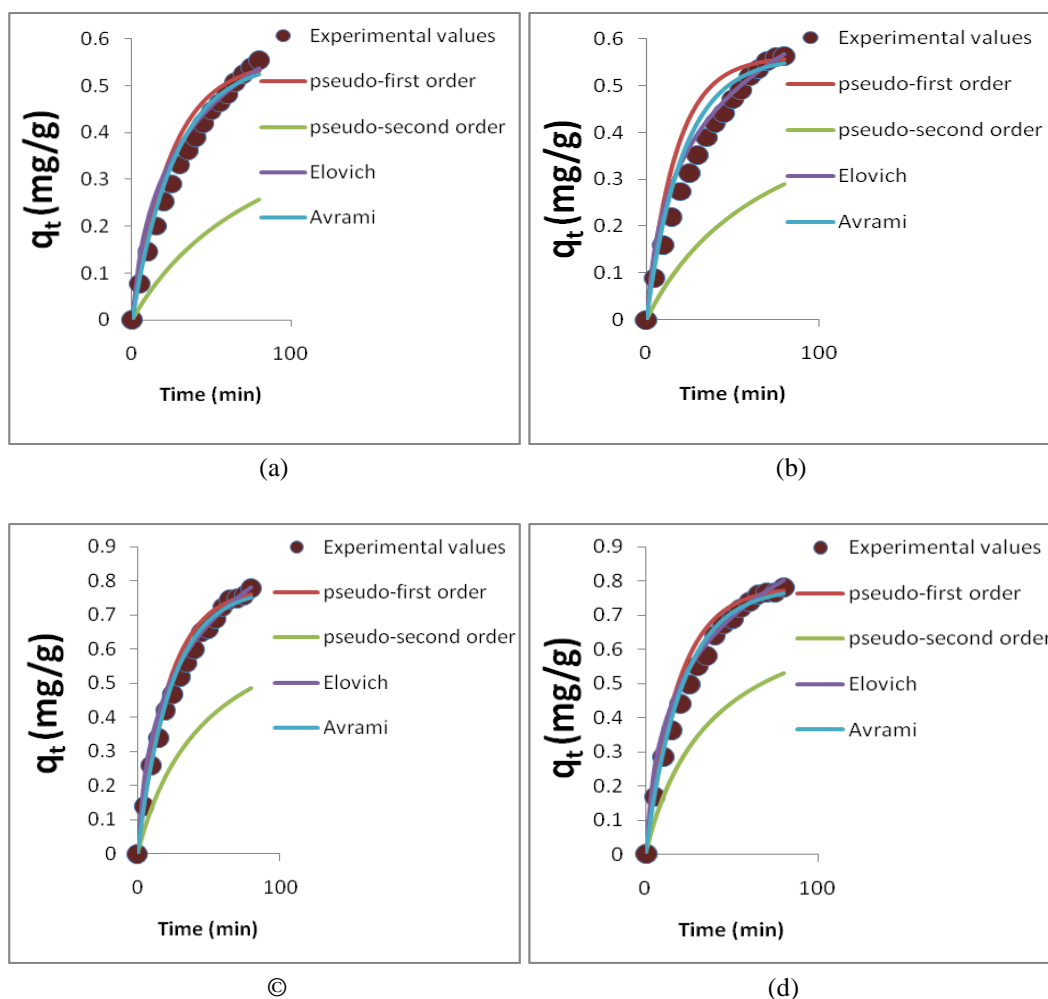


Figure 5: Non-linear plots of the kinetic models at 343K(a), 353K(b), 363K(c), and 373K(d).

Table 6: Intra-particle diffusion model parameters.

Kinetic model	Parameters	Temperature (°C)			
		70	80	90	100
Intra-particle diffusion	$K_{id}(\text{mg/gmin}^{1/2})$	0.071	0.073	0.094	0.092
	c	-0.072	-0.057	-0.020	0.015
	R^2	0.996	0.991	0.980	0.971

3.7 Adsorption isotherms

The equilibrium data obtained from pigments removal from palm oil with activated Karaworo clay, was analyzed using the Langmuir [16], Freundlich [17], Temkin [18], and Dubinin-Radushkevich [19] isotherm models. The linear and non-linear forms of the isotherm models are shown in Table 7, while their linear plots are shown in Figure 6.

Table 7: Linear and Non-Linear forms of isotherm models.

Isotherm model	Non-linear form	Linear form
Langmuir	$q_e = \frac{Q_m K_a C_e}{1 + K_a C_e}$	$\frac{C_e}{q_e} = \frac{1}{K_a Q_m} + \frac{C_e}{Q_m}$
Freundlich	$q_e = K_F C_e^{1/n}$	$\ln q_e = \ln K_F + \frac{1}{n} \ln C_e$
Temkin	$q_e = \frac{RT}{b_T} \ln(K_T C_e)$	$q_e = B_1 \ln K_T + B_1 \ln C_e$
Dubinin-Radushkevich (D-R)	$q_e = Q_m \exp(-\beta \varepsilon^2)$	$\ln q_e = \ln q_m - \beta \varepsilon^2$ $\varepsilon = RT \ln(1 + 1/C_e)$

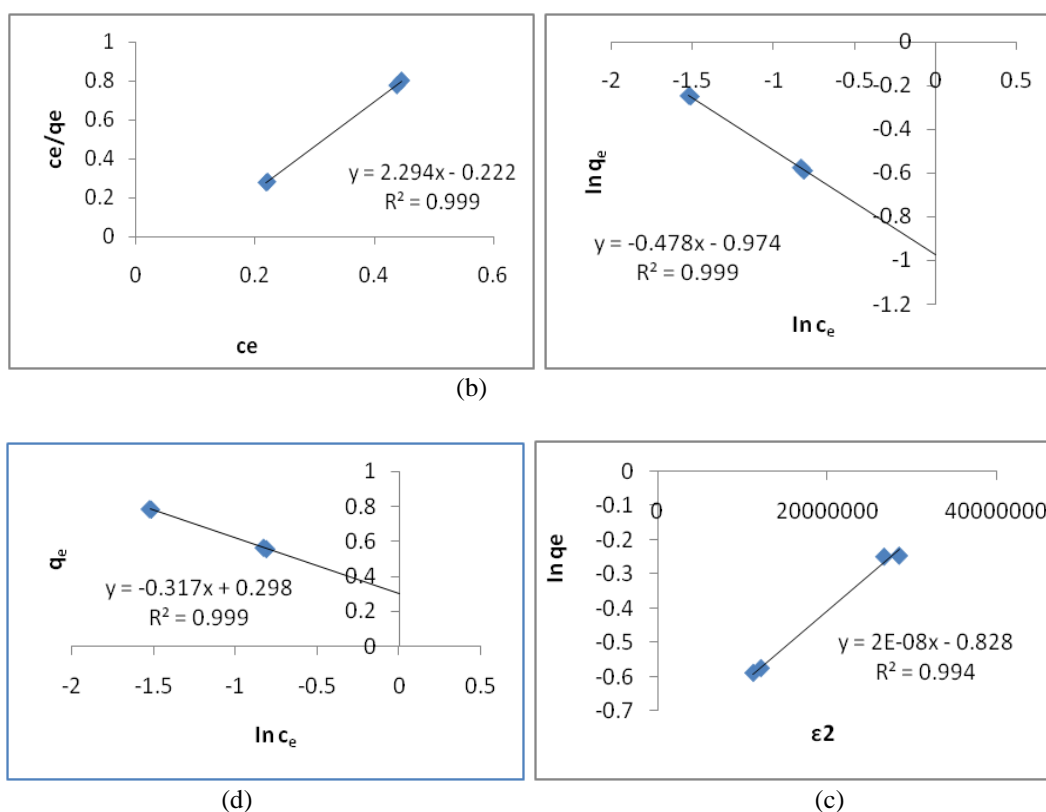


Figure 6: Langmuir (a), Freundlich (b), Temkin (c), and Dubinin-Radushkevich (d) linear plots.

The isotherm parameters estimated from the isotherm plots with the regression coefficients (R^2), are listed in Table 8. The values of R^2 from the isotherms are quite high, with Langmuir, Freundlich, and Temkin isotherms having R^2 values of 0.999. However, the results of the error analysis presented in Table 9 shows that the Freundlich isotherm gives the least error values, indicating that the bleaching process is better described by the Freundlich isotherm.

Table 8: Isotherm parameters for colour pigment removal from palm oil using activated Karaworo kaolinite

Langmuir	Freundlich	Temkin	Dubinin and Radushkevich
$q_m(\text{mg/g}) = 0.436$	$K_F(\text{L/mg}) = 0.378$	$K_T(\text{L/mg}) = 0.391$	$\beta = -2 \times 10^{-8}$
$K_a(\text{L/mg}) = -10.331$	$n = -2.092$	$B_1 = -0.317$	$Q_m(\text{mg/g}) = 0.437$
$R^2 = 0.999$	$R^2 = 0.999$	$R^2 = 0.999$	$R^2 = 0.994$

Table 9: Values of error function of the isotherm models for pigments removal using activated Karaworo kaolinite.

Error function model	Isotherm model			
	Langmuir	Freundlich	Temkin	D-R
ARE(%)	151.394	0.1898	0.2659	52.916
RMSE	1.4186	0.0018	0.0028	0.5703
MPSD(%)	214.8522	0.3020	0.4293	77.7315
S_{RE}	173.6605	0.2194	0.3050	60.6742

3.8 Statistical Analysis of Bleaching Efficiency

To optimize the bleaching efficiency (BE) of the kaolinite sample, response surface methodology (RSM) was used to determine the optimum values of the process variables. The central composite design (CCD) of RSM was used to obtain a quadratic model, consisting of factorial trials and star points to estimate quadratic effects and central points to estimate the pure process variables with bleaching efficiency as response. The process parameters considered include bleaching temperature (A), bleaching time (B) and clay dosage (C). The design plan shown in Table 10 was used to optimize the bleaching efficiency (BE) of Karaworo kaolinite.

Mathematical relationship was generated between the factors (independent variables) and response (dependent variable) using the statistical package Design-Expert 10.0 Trial Version for determining the levels of factors which yield optimum bleaching efficiency. A second order polynomial regression equation that fitted the data is shown in Equation (9).

$$BE (\%) = 86.21 + 4.23*A + 4.03*B + 4.23*C + 0.45*AB - 0.60*AC + 0.025*BC - 3.47*A^2 - 3.48*B^2 - 3.36*C^2 \quad (9)$$

The above equation represents the quantitative effect of the factors (A, B, and C) upon the response (BE). Coefficients with one factor represent the effect of that particular factor, while the coefficients with more than one factor and those with second order terms represent interaction between those factors and the quadratic nature of the phenomena, respectively. Positive sign in front of the terms indicates synergistic effect while negative sign indicates antagonistic effect of the factor. The adequacy of the above proposed model was tested using the Design-Expert model summary statistics. From the model summary statistics, it can be seen that the R-squared, adjusted R-squared and the predicted R-squared values for the quadratic model (0.9966, 0.9935, and 0.9859) showed a better correlation when compared with the 2FI model (0.6244, 0.4510 and 0.0232) and the linear model (0.6204, 0.5493 and 0.4910) as shown in Table 11. The quadratic model also shows a close agreement between the predicted and adjusted R^2 values. This indicates that the quadratic model provides the best relationship between the independent variables and the response.

Table 10: Fractional factorial central composite design for pigments removal from palm oil.

Run	A:Temperature (°C)	B:Time (min)	C:Dosage (g)	Bleaching efficiency (%)	
				Experimental	Predicted
1	45	20	2.5	85.6	86.21
2	45	20	2.5	85.8	86.21
3	60	10	1.5	72.1	72.04
4	30	10	3.5	72.8	72.90
5	60	30	1.5	80.9	80.94
6	45	20	4.18179	84.3	83.82
7	30	30	1.5	70.2	70.38
8	45	20	2.5	85.4	86.21
9	45	20	2.5	86.8	86.21
10	30	10	1.5	63.8	63.28
11	30	30	3.5	79.9	80.10
12	45	3.18207	2.5	69.2	69.58
13	45	20	0.818207	69.3	69.58
14	45	36.8179	2.5	83.7	83.12
15	45	20	2.5	86.8	86.21
16	19.7731	20	2.5	69.2	69.29
17	45	20	2.5	86.8	86.21
18	70.2269	20	2.5	83.8	83.51
19	60	10	3.5	79.3	79.26
20	60	30	3.5	87.6	88.26

From the analysis of variance shown in Table 12, it can be observed that the model F-value (324.27) of the quadratic model is significant. There is only a 0.01% chance that an F-value this large could occur due to noise. Values of "Prob > F" less than 0.0500 indicate model terms are significant. In this case A, B, C, AC, A², B², C² are significant model terms. Values greater than 0.1000 indicate the model terms are not significant. If there are many insignificant model terms (not counting those required to support hierarchy), model reduction may improve the model. Based on this, the insignificant terms of the model are removed and model reduces to Equation (10).

$$BE (\%) = 86.21 + 4.23*A + 4.03*B + 4.23*C - 0.60*AC - 3.47*A^2 - 3.48*B^2 - 3.36*C^2 \quad (10)$$

In terms of actual factor values, the bleaching efficiency is given in Equation (11).

$$BE (\%) = -12.93029 + 1.70849*Temperature + 1.65500* Time + 22.78592*Dosage - 0.0400* Temperature*Dosage - 0.01541* Temperature^2 - 0.034841*Time^2 - 3.36033*Dosage^2 \quad (11)$$

The “Lack of Fit F-value” of 0.75 implies the Lack of Fit is not significant relative to the pure error. There is a 62.23 % chance that a “Lack of Fit F-value” this large could occur due to noise. Non-significant lack of fit is good as it shows that the model is well fitted.

Table 11: Model summary statistics.

Source	Std. Dev.	R-Squared	Adjusted R-Squared	Predicted R-Squared	PRESS	Remark
Linear	5.21	0.6204	0.5493	0.4910	582.89	
2FI	5.75	0.6244	0.4510	0.0232	1118.54	
Quadratic	<u>0.63</u>	<u>0.9966</u>	<u>0.9935</u>	<u>0.9859</u>	<u>16.19</u>	Suggested
Cubic	0.62	0.9980	0.9935	0.9784	24.78	Aliased

Table 12: ANOVA for Response surface reduced quadratic model.

Source	Sum of Squares	df	Mean Square	F Value	p-value Prob > F	
Model	1141.22	9	126.80	324.27	< 0.0001	significant
A- Temperature	244.24	1	244.24	624.58	< 0.0001	
B-Time	221.39	1	221.39	566.15	< 0.0001	
C-Dosage	244.86	1	244.86	626.16	< 0.0001	
AB	1.62	1	1.62	4.14	0.0692	
AC	2.88	1	2.88	7.36	0.0218	
BC	5.00E-003	1	5.000E-003	0.013	0.9122	
A ²	173.16	1	173.16	442.83	< 0.0001	
B ²	174.94	1	174.94	447.35	< 0.0001	
C ²	162.73	1	162.73	416.14	< 0.0001	
Residual	3.91	10	0.39			
Lack of Fit	1.67	5	0.33	0.75	0.6223	not significant
Pure Error	2.24	5	0.45			
Cor Total	1145.13	19				

The coefficient of variation (CV) value of 0.79 illustrate that the model can be considered reasonably reproducible [20]. The signal to noise ratio which is given as the value of the adequate precision is 56.491 as shown in Table 13. It indicates that an adequate relationship of signal to noise ratio exists and that the result can be used to navigate the design space.

Table 13: Summary of regression values

Std. Dev.	Mean	C.V. %	PRESS	Adeq. Precision
0.63	79.16	0.79	16.19	56.491

The experimental data were also analyzed to check the correlation between the experimental and predicted bleaching efficiencies as shown in Figure 7(a). It can be seen from Figure 7(a) that the data points on the plot were reasonably distributed near to the straight line, indicating a good relationship between the experimental and predicted values of the response and further shows that the underlying assumptions of the above analysis were appropriate [21, 22].

3.9 Response surface plots

The 3D response surface plots which represent the interactive effects of two of the process variables on the bleaching efficiency while keeping the other factors at their central (0) level are shown in Figure 7(b-d). The influence of bleaching temperature and bleaching time on the bleaching efficiency of the clay is shown in Figure 7b. As the bleaching time increased from 10 to 25 minutes, the bleaching efficiency increased from 79 to 87.5 %, while as the bleaching temperature increased from 30 °C to 54 °C, the bleaching efficiency of the clay increased from 78 % to 87.5 % as seen in Figure 7b. This linear relationship is as a result of increase in kinetic energy with higher temperature.

A plot for the combined interactive effects of bleaching temperature and clay dosage on the removal of pigments from palm oil is shown in Figure 7c. As the clay dosage increased from 1.5 to 3.0 g, the bleaching efficiency increased from 80 % to 87.5 %, while as the bleaching temperature increased from 30 to 54 °C, the bleaching efficiency also increased from 80 to 87.5 %. The effect of bleaching time and clay dosage on the bleaching efficiency is shown in Figure 7d. As the bleaching time increased from 10 to 25 minutes, the bleaching efficiency increased from 79.5 % to 87.5 %, while as the clay dosage increased from 1.5g to 3.0g, the bleaching efficiency increased from 79 % to 87.5 %.

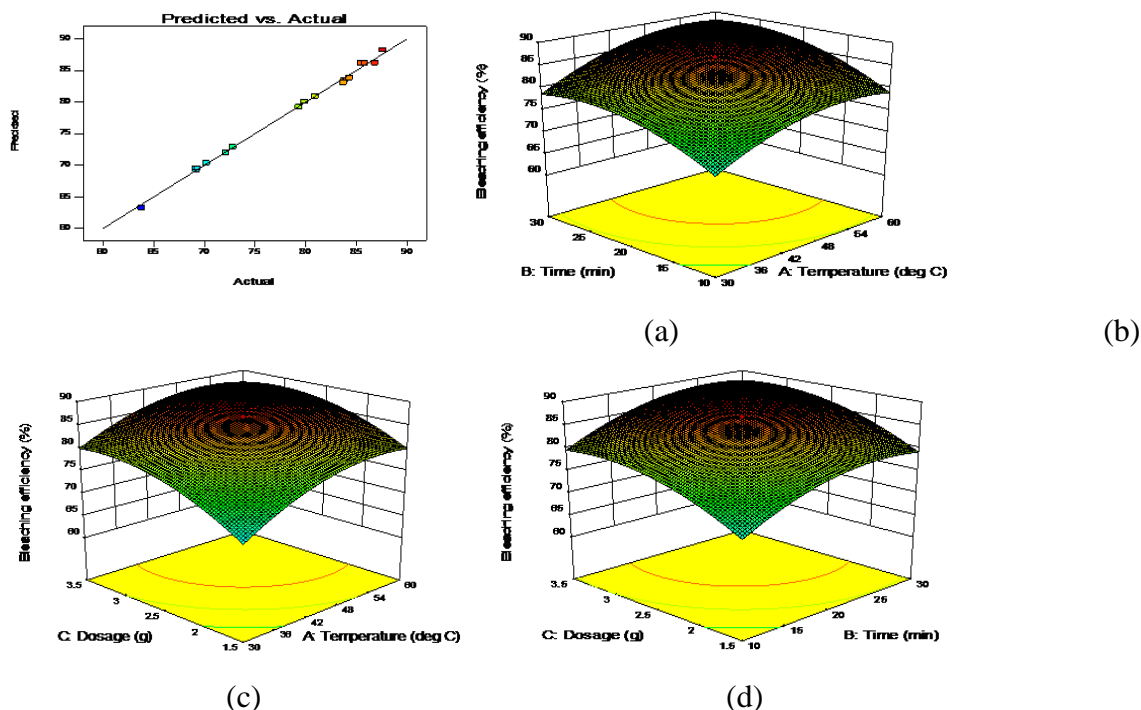


Figure 7: Plot of predicted vs. experimental values (a) and 3D response surface plots (b-d).

3.10 Numerical Optimization Using Response Surface Methodology and Genetic Algorithm

The optimization exercise for the bleaching process was conducted separately using the optimization tools of the central composite design (CCD) of design expert software and genetic algorithm of matlab. Equation (11) was solved for the best solutions such that the response (BE) was maximized within the

design space. A usual approach, which involves selecting the best solution based on economic considerations, was adopted. The developed model from the CCD predicted optimum conditions of 60°C bleaching temperature, 30 minutes bleaching time and 3.5g clay dosage. At the above conditions, an optimum bleaching efficiency of 88.26% was predicted by the software. The GA optimization parameters were determined by a trial-and-error. The best conditions were selected in which the initial range was [1,100], the elite count and crossover fraction were, respectively, equal to 2 and 0.8, the mutation, scaling, selection, and crossover functions were respectively selected as adaptive feasible, proportional, stochastic uniform and scattered. Figure 8a shows the average distance between the individuals for each generation. Figure 8b shows the mean value of the fitness function of generation 200, which is 82.59%. The optimal values for the independent variables for the bleaching temperature, bleaching time and clay dosage were equal to 60°C, 30 minutes, and 3.5g, respectively (Figure 8c). By performing three different experiments at the above conditions, the bleaching efficiency was validated as 84.26%.

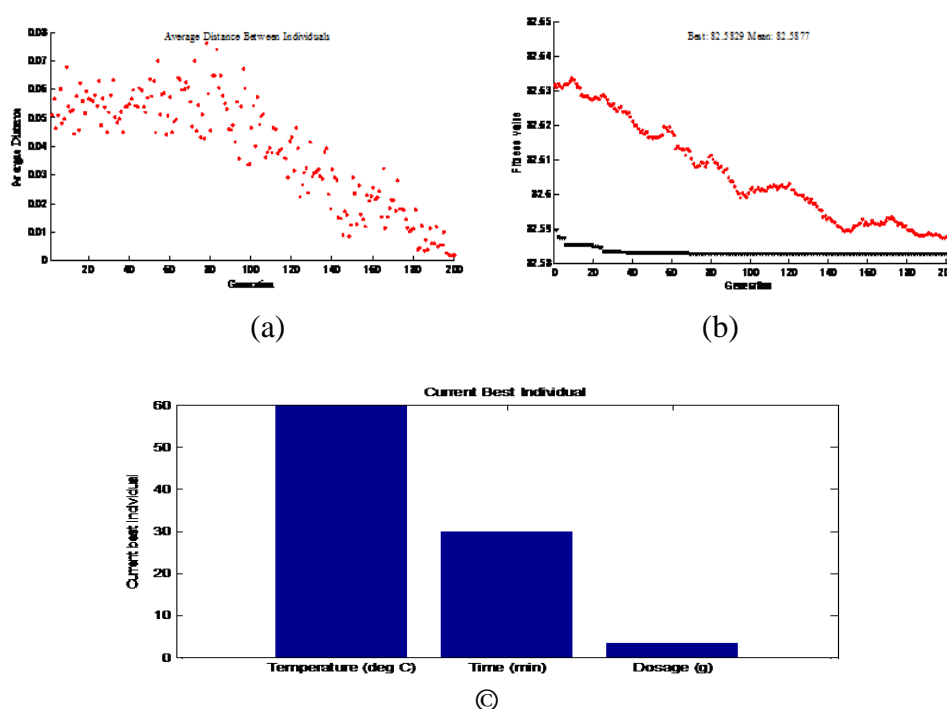


Figure 8: The obtained charts for the obtained points by GAs: (a) average distance between the individuals in each generation (b) the best value for the fitness function and (c) the optimal values obtained for the fitness function's independent variables.

Conclusion

The results obtained in this study indicate the suitability of activated Karaworo clay for the removal of pigments from palm oil. The uptake of pigments onto the clay was controlled by the acid concentration during clay activation, dosage, and temperature. The maximum bleaching efficiency was recorded at 7M HCl concentration, 4g clay dosage and 100°C. The obtained data fitted the Freundlich model. The pseudo-second order kinetic model described the adsorption process with high correlation coefficients better than other kinetic models. Adsorption mechanism studies showed that the intra-particle diffusion was not the sole determinant of the mechanism of the bleaching process. About 88.26% pigments removal was predicted at 60°C bleaching temperature, 30 minutes bleaching time and 3.5g clay dosage, using response surface methodology. At the above conditions, about 82.59% pigments removal were predicted using genetic algorithm.

References

1. S. Palaniappan, A. Proctor, Evaluation of soy oil lutein isotherms obtained with selected adsorbents in hexane miscellas, *Journal of the American Oil Chemists Society* 68(1991) 79-82. <https://doi.org/10.1007/BF02662321>
2. O. Lacin, E. Sayan, E. G. Kirali, Optimization of acid- activated bentonites on bleaching of cotton oil, *Journal of the Chemical Society of Pakistan* 35(2013)1053 – 1059.
3. J. T. Nwabanne, F. C. Ekwu, Decolourization of palm oil by Nigerian local clay: A study of adsorption isotherms and bleaching kinetics, *International Journal of Multidisciplinary Sciences and Engineering* 4 (2013) 20-25.
4. M. Z. Alam, S. A. Muyibi, J. Toramae, Statistical optimization of adsorption processes for removal of a 2,4-dichlorophenol by activated carbon derived from oil palm empty fruit bunches, *Journal of Environmental Sciences* 19(2007) 674 – 677. [https://doi.org/10.1016/S1001-0742\(07\)60113-2](https://doi.org/10.1016/S1001-0742(07)60113-2)
5. E. Betiku, S. S. Okunsolawo, S. O. Ajala, O. S. Odedele, Performance evaluation of artificial neural network coupled with genetic algorithm and response surface methodology in modeling and optimization of biodiesel production process parameters from shea tree (*Vitellaria paradoxa*) nut butter, *Renewable energy* 76(2015) 408-417. <http://dx.doi.org/10.1016/j.renene.2014.11.049>
6. D. Bas, I. H. Boyaci, Modeling and Optimization II: Comparison of estimation capabilities of response surface methodology with artificial neural networks in a biochemical reaction, *Journal of Food Engineering* 78(3)(2007) 846-54.
7. D. E. Goldberg, *Genetic Algorithms in Search, Optimization, and Machine Learning*, Addison-Wesley, Reading, 1989. <https://doi.org/10.1023/A:1022602019183>
8. E. Fayyazi, B. Ghobadian, G. Najafi, B. Hosseinzadeh, R. Mamat, J. Hosseinzadeh, An Ultrasound-Assisted System for the Optimization of Biodiesel Production from Chicken Fat Oil Using a Genetic Algorithm and Response Surface Methodology, *Ultrasonics Sonochemistry* 26(2015) 312-320. <http://doi.org/10.1016/j.ultsonch.2015.03.007>
9. A. Sharma, R. Patani, A. Aggarwal, Software testing using genetic algorithms. *International Journal of Computer Science And Engineering Survey* 7(2) (2016) 21–33. <http://doi.org/10.5121/ijcses.2016.7203.21>
10. S. Oreski, G. Oreski, Genetic algorithm-based heuristic for feature selection in credit risk assessment. *Expert Systems With Applications* 41(2014) 2025-2064. <http://doi.org/10.1016/j.eswa.2013.09.004>
11. R. O. Ajemba, O. D. Onukwuli, Adsorptive removal of colour pigment from palm oil using acid activated Nteje clay: Kinetics, Equilibrium and Thermodynamics, *Physicochemical Problems of Mineral Processing* 49 (2013), 369 – 381. <http://dx.doi.org/10.5277/ppmp130133>
12. V. N. Okafor, I. A. Nnanwube, J. I. Obibuenyi, O. D. Onukwuli, R. O. Ajemba, Removal of pigments from palm oil using activated Ibusa kaolinite: Equilibrium, Kinetic and Thermodynamic Studies, *Journal of Minerals and Materials Characterization and Engineering* 7 (2019) 157-170. <http://doi:10.4236/jmmce.2019.74012>
13. A. L. Prasad, T. Santhi, S. Mononmani, Recent development in preparation of activated carbons by microwave: Study of residual errors. *Arabian Journal of Chemistry* 8(2015)343-354. <http://dx.doi.org/10.1016/j.arabjc.2011.01.020>
14. K. A. Bakhtyar, A. A. Muhammad, J. J. Karim, Acid activation and bleaching capacity of some local clays for decolourizing used oils, *Asian Journal of Chemistry* 23 (2011) 113-122.

15. M. M. El-Halwany, Study of adsorption isotherms and kinetic models for methylene blue adsorption on activated carbon developed from Egyptian rice hull(Part II), *Desalination*, 250 (2010) 208 – 213. <http://doi:10.1016/j.desal.2008.07.030>
16. T. A. Khan, S. Dahiya, I. Ali., Use of kaolinite as adsorbent: Equilibrium, dynamics and thermodynamic studies on the adsorption of Rhodamine B from aqueous solution, *Applied Clay Science* 69 (2012) 58-66. <http://dx.doi.org/10.1016/j.clay.2012.09.001>
17. S. K. Yadav, D. K. Singh, S. Sinha, Chemical carbonization of papaya seed originated charcoals for sorption of Pb(II) from aqueous solution, *Journal of Environmental Chemical Engineering* 2 (2014) 9 -19. <http://dx.doi.org/10.1016/j.jece.2013.10.019>
18. M. J. Temkin, V. Pyzhev, Recent modifications to Langmuir isotherms, *Acta Physicochimica USSR* 12 (1940) 217-225.
19. M. M. Dubinin, L. V. Radushkevich, Equation of the characteristic curve of activated charcoal, *Proceedings of the National academy of Sciences USSR* 55(1947), 331-333.
20. G. Chen, J. Chen, C. Srinivasakannan, J. Peng, Application of response surface methodology for optimization of the synthesis of synthetic rutile from titania slag. *Applied Surface Science* 258(2011)3068-3073. <https://doi.org/10.1016/j.apsusc.2011.11.039>
21. R. O. Ajemba, O. D. Onukwuli, Determination of the optimum dissolution conditions of Ukpor clay in hydrochloric acid using Response Surface Methodology. *International Journal of Engineering Research & Applications* 2(5) (2012)732-742.
22. I. A. Nnanwube, O. D. Onukwuli, J. I. Obibuenyi, V. N. Okafor, R. O. Ajemba, Optimization of colour pigments removal from palm oil using activated Ogbunike kaolinite. *Sigma Journal of Engineering and Natural Sciences* 38(1) (2020)253-263.

(2020) ; <http://www.jmaterenvirosci.com>